Research Square

Preprints are preliminary reports that have not undergone peer review.
They should not be considered conclusive, used to inform clinical practice,
or referenced by the media as validated information.

Early 7,8-Dihydroxyflavone administration ameliorates synaptic and behavioral deficits in the young FXS animal model by acting on BDNF-TrkB pathway

Yu-shan Chen
Wuhan University of Science and Technology
Si-ming Zhang
Wuhan University of Science and Technology
Qiong Zhu
Wuhan University of Science and Technology
Chao-xiong Yue
Wuhan University of Science and Technology
Peng Xiang
Wuhan University of Science and Technology
Jin-quan Li
Wuhan University of Science and Technology
Zhen Wei
Wuhan University of Science and Technology
Yan Zeng (zengyan68@wust.edu.cn)
Wuhan University of Science and Technology https://orcid.org/0000-0002-5119-5448

Research Article

Keywords: Fragile X syndrome, Brain-derived neurotrophic factor, Tyrosine kinase B receptor, 7, 8-Dhydroxyflavone, dendritic spine, learning and memory

Posted Date: September 28th, 2022

DOI: https://doi.org/10.21203/rs.3.rs-2080048/v1

License: This work is licensed under a Creative Commons Attribution 4.0 International License.
Read Full License

Version of Record: A version of this preprint was published at Molecular Neurobiology on January 21st, 2023. See the published version at https://doi.org/10.1007/s12035-023-03226-w.

Abstract

Fragile X syndrome (FXS) is the leading inherited form of intellectual disability and the most common known cause of autism spectrum disorders. FXS patients exhibit severe syndromic features and behavioral alterations, including anxiety, hyperactivity, impulsivity, and aggression, in addition to cognitive impairment and seizures. At present, there are no effective treatments or cures for FXS. Previously, we have found the divergence of BDNF-TrkB signaling trajectories is associated with spine defects in early postnatal developmental stages of *Fmr1* KO mice. Here, young fragile X mice were intraperitoneal injection of 7,8-Dihydroxyflavone (7,8-DHF), which is a high affinity tropomyosin receptor kinase B (TrkB) agonist. 7,8-DHF ameliorated morphological abnormities in dendritic spine and synaptic structure, and rescued synaptic and hippocampus-dependent cognitive dysfunction in young FXS mice. These observed improvement of 7,8-DHF involved decreased protein levels of BDNF, p-TrkB^{Y816}, p-PLCγ, and p-CaMKII in the hippocampus. In addition, 7,8-DHF intervention in primary hippocampal neurons increased p-TrkB^{Y816} through activating the PLCγ1-CaMKII signaling pathway leading to improvement of neuronal morphology. This study is the first to account for early life synaptic impairments, neuronal morphological and cognitive delays in FXS in response to the abnormal BDNF-TrkB pathway. Present studies provide novel evidences about the effective early intervention in FXS mice at developmental stages as a strategy to produce powerful impacts on neural development, synaptic plasticity and behaviors.

Introduction

Fragile X syndrome (FXS) is a prevalent, inherited neurodevelopmental disorder and is associated with learning disabilities, seizures, hyperactivity, and autism [1]. In the vast majority of cases, FXS is caused by excessive expansions of a noncoding CGG repeat in the fragile X mental retardation 1 (*Fmr1*) gene, with transcriptional silencing of *Fmr1* and a consequent reduction of *Fmr1* encoded protein (FMRP) [2]. FMRP deficiency affects the translational regulation of multiple proteins involved in regulation of dendritic morphology, synaptic function and behavioral phenotypes including cognitive deficits, anxiety, impaired social interactions, hyperactivity, and aggression [3, 4]. In light of the genetic disorder of neurodevelopment, behavioral and neuronal abnormalities in FXS are often thought to be closely associated with biological and molecular mechanisms. Especially, proteins altered in FXS are implicated in signaling pathways that regulate dendritic spine development [5–8], leading abnormally long and thin dendritic spines in the brains of individuals with FXS and the *Fmr1* knockout (KO) mice [7, 9]. However, mechanistic insights into the molecular components of these abnormalities remain limited.

Among various growth-promoting signals implicated in the regulation of neuronal morphogenesis and synapse formation, brain-derived neurotrophic factor (BDNF) is one of the strongest candidates to regulate the formation and maturation of dendritic spines in postnatal development [10, 11]. BDNF signaling is required for normal brain function in both the developing and mature nervous system [12, 13]. Moreover, BDNF and its high-affinity receptor tropomyosin-related kinase B (TrkB) are essential in various processes associated with functional and structural synaptic plasticity, learning, and memory [14, 15, 13]. Although the importance of BDNF-TrkB for neuronal morphogenesis and synaptic plasticity is well

established, its putative implication in FXS pathologies is less clear. Several studies indicate that BDNF protein production is altered in the brain of *Fmr1* KO mice and several FMRP functions are modulated by BDNF signaling [16–18]. The recent study has also shown that the expression profile of BDNF during early phases of neuronal development and we found the correlation between BDNF-TrkB signaling and mature spines in young FXS mice [19]. In this sense, BDNF-TrkB pathway impairments during development maybe the key mechanisms underlying abnormal dendritic spine morphogenesis and cognitive dysfunction in FXS.

Several previously published studies support that applying the intervention strategies in the early developmental stages is critical to ameliorate pathological phenotypes of neurodevelopmental disorders [20–22]. Early intervention strategies during critical developmental periods exhibit successful improvement in ASD before major symptoms develop [23–25, 20]. For example, early inhibition of group1 mGlu signaling at development stage, but not in adulthood, could rescue dendritic spine abnormalities in *Fmr1* KO mice [26]. Early postnatal low-dose VPA treatment improve ASD-like behaviors associated with sustained rescue of repetitive behavior and social deficits in *shank3ab* KO zebrafish model [25]. Administration with lovastatin during the early age of *Fmr1* KO rats was able to correct associative learning deficits and also has lasting beneficial effects [23]. Moreover, clinical studies have demonstrated early intervention of problem behavior marked beneficial effects in children with FXS and ASD [20, 27–30]. Hence, the mechanism underlying the effectiveness of early intervention for FXS is warranted further examination.

The present study examined the effect of early intervention psychopharmacological administration with TrkB agonist 7,8-DHF on FXS mouse model at the critical developmental stages at morphological, behavior, biochemical, molecular and physiological levels. The results showed that early treatments with 7,8-DHF can rescue spatial and fear memory dysfunction, and alleviate immature dendritic spines, hippocampal synaptic structure and plasticity impairment in *Fmr1* KO mice. These effects were associated with augmented BDNF levels and TrkB-PLCγ1-CaMK signals. *In vitro* experiments also showed that TrkB or PLCγ agonists promoted dendrite branching and lengthening in cultured hippocampus neurons. In all, this study supports the notion that early pharmacological interventions with 7,8-DHF ameliorates the behavioral and synaptic abnormalities of *Fmr1* KO mice at early ages by acting on BDNF-TrkB pathway.

Materials And Methods

Animals

All procedures were approved by the Wuhan University of Science and Technology (WUST, Wuhan, China) ethics committee with the number IACUC-2017032. FVB.129P2 *Fmr1* KO and WT mice were maintained on a 12h dark/light cycle at 21–23°C and 40–60% humidity facility with free access to food and water at the animal center of WUST. Animals were 2-week-old at the beginning of the experimental manipulation.

Mice were allocated arbitrarily into different groups and the number of each group is indicated in figure legends.

Drug treatments

7,8-DHF was obtained from Sigma Aldrich (St Louis, MO) and dissolved in 17% DMSO and subsequently on sterile saline (vehicle). *Fmr1* KO and wild-type control mice at P14 were administered 5 mg/kg 7,8-DHF through intraperitoneal injections once daily for 16 consecutive days. To determine the appropriate dose, mice were weighted daily. Untreated groups received the same volume of vehicle with the same schedule. Animals were sacrificed and subjected to histological and biochemical analysis after the last administration. Behavioral tests were performed at P60. For *in vitro* experiments, primary neurons were treated with 7,8-DHF (0.5 μM, 1 μM, or 5 μM) at DIV 4 for 3 days. We used the inhibitor K252a (50 nM or 100 nM) at DIV 6 for 24h or PLCγ agonist m-3M3FBS (25 μM) at DIV 5 for 3h. After treatment, we analyzed neural complexity including dendritic length and branches using immunofluorescent confocal microscopy.

Primary hippocampal neuron culture

Primary hippocampal neuron cultures from neonatal mice were prepared as previously described [31]. Briefly, euthanize the mouse and then gently remove the intact brain into dissection medium. The hippocampus was dissected and digested with D-Hanks (Gibco, USA) containing 0.25% trypsin (Gibco, USA) for 10 min and then dissociated by repeated trituration. Dissociated neurons were plated at a concentration of 15×10^4 cells/cm^2 an appropriate density ($1–7\times10^5$ per mL) on plates precoated with poly-L-lysine-coated. After being incubated in a 37 ºC incubator with 5% CO_2 for 4h, neurons were covered by Neurobasal medium with 2% B27 and 1% L-glutamine. Half of the old medium were replaced twice every week.

Immunocytochemistry and confocal imaging

Cells fixed with 4% paraformaldehyde were rinsed three times with 0.1 M PBS. Fixed cells were permeabilized and then blocked with 0.05% Triton X-100 containing 5% bovine serum albumin (BSA) at room temperature for 1 h. After incubated with primary antibodies overnight, cells were washed with PBS for three times and then incubated with fluorescent secondary antibodies for 2h. Slices were mounted and then covered with Mowiol and coverslips. Visual inspection and image acquisition were done using a FV1000 confocal-IX81 microscope (FluoView1000-IX81, Olympus, Tokyo, Japan). At least one entire neuron was presented on the field of vision. To quantify the total length of dendrite trees and number of dendrite branches, at least 50 neurons randomly selected from 5 independent cultures per condition were analyzed. Automated quantification of neurite length and branches was performed using Image J software. All measurements were performed in a blinded way.

Western blotting

Hippocampal total extracts and cultured neurons from mice were lysed in RIPA lysis buffer (Thermo Fisher Scientific) to collect protein samples. Western blotting was performed as described previously [5].

Immunoblots were probed with the primary and secondary antibodies as shown in Table S1. The immunoreactive membranes were imaged using Western Blotting Luminol Reagent (Bio-Red,1705060) and quantified by Image J.

Golgi-Cox staining and dendritic spine analysis

The procedure for Golgi staining was adapted from Cheng et al. previously [32]. Neurons were stained with Golgi using the FD Rapid Golgi Staining Kit (FD Neurotechnology, Columbia, MD, USA). After the staining, we used Olympus BX51WI Microscope to obtain bright-field images of pyramidal neurons in CA1 area of hippocampus and qualified the dendritic spines in 3–9 neurons/mice (5 segments/neuron) by Neurolucida software 9.0 (MicroBright Field, Williston, USA). Dendritic spines were classified into 4 categories mushroom, stubby, branched and thin based on their shape as reported previously [33]. The percentage of spines in each classification of the total spines was analyzed.

Transmission electron microscopy (TEM)

TEM experiments were conducted as the previous studies [19, 34]. Samples were immersed in 1% osmium tetraoxide in PBS for 2h and then dehydrated in graded ethanol, and embedded in epoxy resin. The 90 nm-thickness ultrathin sections cutting by Leica ultracut ultramicrotome were counterstained using uranyl acetate and lead citrate. Electron micrographs were taken by an electron microscope (Tecnai G2 20 TWIN, FEI, USA). Synapse were detected by a vesicle-filled presynaptic structure and postsynaptic density (PSD) in the target area. We quantified the synaptic density, PSD thickness, width of the synaptic cleft and length of the synaptic active zone for at least 60–80 electron microscopic images per group.

Slice electrophysiology

Slice preparation and electrophysiological recordings were the same as previously described [35, 36]. Vehicle or 7,8-DHF treated mice were decapitated and the brains were quickly removed and immersed in ice-cold artificial cerebrospinal fluid (ACSF, in mM: 124 NaCl, 3 KCl, 1.25 KH_2PO_4, 26 $NaHCO_3$, 2 $CaCl_2$, 1 $MgCl_2$, and 10 glucose, pH = 7.4 ± 0.5) continuously bubbled with 95% O_2 and 5% CO_2. Hippocampal slices (400 μm) were prepared by vibratome slicing and incubated in the recovery chamber (0.5h at 34–36°C and 1h at room temperature). Then acute slices were transferred to a recording chamber perfused with ACSF (34°C) at 2 ml/min. Basal synaptic transmission (BST) was evaluated by increasing the stimulating intensity and field excitatory postsynaptic potentials (fEPSPs) was measured using an input-output curve. On the basis of this curve, the stimulus was adjusted to elicit a fEPSP with approximately half the maximum slope. A 64-channel multielectrode (MED64) system (Alpha MED Science, Tokyo, Japan) was used to record fEPSPs [37]. Long-term depression (LTD) was induced by low-frequency stimulation consisting of 900 pulses at 1 Hz [38–40].

Morris water maze test

Morris water maze (MWM) is commonly used to assess spatial learning and memory [5]. A circular white tank (1.2 m diameter) was filled with 0.5 m water (22 ± 2°C) and divided into four quadrants. A 10 cm-diameter circular platform was placed in the middle of the third quadrant 2–4 cm beneath the water

surface. Mice were trained for 5 consecutive days, and the probe trial was performed on day 6. During training, a mouse was randomly placed in one of the four quadrants, and allowed for the mouse to find the hidden platform (60 s-cut-off). On day 6, the platform was removed and the probe trial was performed. Time spending in the target quadrant was measured. After the probe trial, swimming speed and latency to reach the visible platform were determined. All trials were recorded by the EthoVision automated tracking system (EthoVision, Noldus Information Technology, Netherlands).

Fear conditioning test

Fear conditioning paradigm was slightly modified and performed as previously described [5]. During the training phase, mice were allowed to adapt to the training chamber for 180 s and then were delivered with a tone (75 dB, 2500 Hz) for 30s and an immediate 2 s, 0.75 mA foot shock. Three training sessions were performed. Freezing behavior, defined as the complete absence of movement except for respiration, was measured, and the data were analyzed using the Freezeframe software (Actimetrics, IL, USA). On day two, mice were returned to the fear conditioning chamber for180 s with no tone or shock presented. Two hours later, cued fear memory was tested and mice were placed in the same chamber modified with decorations of various shapes and a novel floor. Freezing behavior 180 s before and after the presentation of the tone was measured.

Statistical analysis

All data were expressed as means ± standard error of measurement (SEM). Data of all experiments were analyzed using Prism software (GraphPad 9.2). For the comparison between two groups, differences were analyzed with an unpaired two-tailed Student's t test. One-way ANOVA and two-way ANOVA followed by Bonferroni's post hoc tests were used for multiple comparisons. Two-sided for p-values < 0.05 were considered statistically significant.

Results

TrkB and PLCγ agonists improve neuronal morphology in primary neurons obtained from Fmr1 KO mice

Since TrkB and PLCγ activation is down regulated and may cause the aberrant dendritic spines in *Fmr1* KO mice [19], we asked if TrkB and PLCγ agonists could improve hippocampal neuronal morphology *in vitro*. Then we examined the dendritic length and branches in neurons treated with or without 7,8-DHF (TrkB agonist), m-3M3FBS (PLCγ agonist) or K252a (TrkB inhibitor). Firstly, we treated WT and KO primary neurons at 4 days *in vitro* (DIV 4) with 0.5, 1 or 5μM 7,8-DHF for 3 days. Additionally, to ensure that the morphological effect was specific through TrkB, we used the inhibitor K252a (50 nM or 100 nM) at DIV 7 for 24h.We observed that branches and total dendritic length were significantly decreased in KO cultures compared with WT cultures (branches: df = 98, t = 2.145,p = 0.034; length: df = 98, t = 2.115, p = 0.037). When treated with 0.5 μM 7,8 DHF, cultures KO cultures exhibited a significant increase in numbers of branches and dendritic length compared to vehicle-KO (branches: df = 98, t = 9.777, p < 0.001; length: df = 98, t = 14.35, p < 0.001). Whereas treated with 100 nM K252a, both KO an WT cultures showed decreased dendritic length and reduced branches (branches: df = 98, t = 4.951, p < 0.001; length: df = 98, t

= 4.488, p < 0.001) (Fig. 1A, 1B, and 1C), which suggest the pivotal role of TrkB acting on neuron mature. To further examine the effect of TrkB downstream activation in neuron maturation, we chose PLCγ, which is decreased in *Fmr1* KO mice. PLCγ agonist 25μM m-3M3FBS, when used at DIV 5 for 3h, significantly increased the number of branches and dendritic length in vehicle-KO mice to levels that comparable to the vehicle-WT group (branches: df = 98, t = 5.648, p < 0.001; length: df = 98, t = 7.604, p < 0.001, Fig. 3D, 3E, and 3F). Two-way ANOVA of branches and dendritic length showed a main effect of genotype [F (1,196) = 10.20, p = 0.002; F (1,196) = 14.02, p < 0.001], treatment [F (1,196) = 9.692, p = 0.002; F(1,196) = 131.1, p < 0.001], and genotype×treatment interaction [F (1,196) = 7.522, p = 0.007; F(1,196) = 5.829, p = 0.017]. Therefore, activation of TrkB-PLCγ pathway contributes to enhanced neuron maturation in *Fmr1* KO mice.

TrkB phosphorylation and downstream PLCγ-CaMKII signaling pathway are normalized by TrkB agonist 7,8-DHF in Fmr1 KO mice

Our previous study has suggested that BDNF/TrkB-PLCγ1-CaMKII signaling is downregulated at the early stages of postnatal development in *Fmr1* KO mice [19]. To investigate whether aberrant TrkB and the downstream signaling pathways would be rescued by TrkB agonist 7,8-DHF, we first studied the activation status of p-TrkB, p-PLCγ, and p-CaMKII after treating P14 mice with 5 mg/kg 7,8-DHF daily for continuous 16 days (Fig. 2A). Quantitative analysis revealed higher activation of p-TrkBY^{816} in 7,8-DHF-treated *Fmr1* KO mice than in vehicle-treated KO mice, whereas p-TrkBY^{515} kept unchanged (Fig. 2A and 2B). Two-way ANOVA of p-TrkBY^{816} levels showed a genotype × treatment interaction [F(1,28) = 5.727, p = 0.024], a main effect of genotype [F(1,28) = 4.410, p = 0.0449], and a main effect of treatment [F(1,28) = 9.308, p = 0.005]. In addition, levels of p-PLCγ and p-CaMKII were significantly increased in 7,8-DHF-treated KO mice compared with vehicle-treated KO mice (Fig. 2A and 2C). Two-way ANOVA of p-PLCγ and p-CaMKII levels showed a genotype × treatment interaction [F(1,28) = 9.578, p = 0.004; F(1,28) = 4.646, p = 0.040, respectively], a main effect of genotype [F(1,28) = 14.79, p < 0.001; F(1,28) = 5.300, p = 0.029, respectively], and a main effect of treatment [F(1,28) = 4.919, p = 0.035; F(1,28) = 4.313, p = 0.047, respectively]. Collectively, these results indicate that TrkB agonist 7,8-DHF rescued the deficient TrkB-PLCγ-CaMKII signaling in *Fmr1* KO mice.

Synaptic loss and synaptic plasticity in Fmr1 KO mice were restored by TrkB agonist 7,8-DHF

To test whether TrkB agonist 7,8-DHF also restore synaptic structure and function in *Fmr1* KO mice since it rescued deficient hippocampal TrkB-PLCγ-CaMKII signaling, we first examined spine density of pyramidal neurons in hippocampal CA1 using Golgi staining. Dendritic spines were classified into the following categories: mushroom, stubby, thin and branched [33, 41]. Vehicle-KO mice exhibited markedly increased thin, filopodia-like spines and decreased mushroom spines compared with vehicle-WT mice, which was noticeably rescued by 7,8-DHF treatment (Fig. 3A and 3B). Two-way ANOVA of thin and mushroom percentage showed a genotype × treatment interaction [F (1,16) = 28.48, p < 0.001; F (1,16) = 16.64, p = 0.002, respectively], a main effect of genotype [F (1,28) = 84.82, p < 0.001; F(1,28) = 174.6, p < 0.001, respectively], and a main effect of treatment [F(1,28) = 18.56, p < 0.001; F(1,28) = 30.68, p < 0.001,

respectively]. The numbers of stubby spines in CA1 regions were similar between vehicle-WT and vehicle-KO mice. The length of dendritic spines was significantly increased in vehicle-KO mice compared to vehicle-WT mice but was remedied by 7,8-DHF treatment (Fig. 3A and 3C). Two-way ANOVA of spine length showed a genotype × treatment interaction [$F(1,16) = 10.70$, $p = 0.005$], a main effect of genotype [$F(1,16) = 72.30$, $p < 0.001$], and a main effect of treatment [$F(1,16) = 24.06$, $p < 0.001$].

We then utilized transmission electron microscopy (TEM) to compare the synaptic density and structure between groups in hippocampal CA1 of FXS mice. We found that Vehicle-KO hippocampus have less synapse, thinner PSD and shorter synaptic active zone (Fig. 3E, 3G and 3H) but wider synaptic cleft than Vehicle-WT group (Fig. 3F). Notably, 7,8-DHF treatment was sufficient to revert the decrease of synaptic density, PSD thickness, and length of the synaptic active zone, and also revert the increase of synaptic cleft width (Fig. 3E, 3F, 3G and 3H). Two-way ANOVA of synaptic density, PSD thickness, length of the synaptic active zone, and synaptic cleft width showed a genotype × treatment interaction [$F(1,361) = 329.2$, $p < 0.001$; $F(1,361) = 3.38$, $p = 0.067$; $F(1,361) = 69.35$; $F(1,361) = 17.22$, $p < 0.001$, respectively], a main effect of genotype [$F(1,361) = 38.55$, $p < 0.001$; $F(1,361) = 37.05$, $p < 0.001$; $F(1,361) = 96.03$, $p < 0.001$; $F(1,361) = 65.53$, $p < 0.001$,respectively], and a main effect of treatment [$F(1,361) = 241.2$, $p < 0.001$; $F(1,361) = 17.66$, $p < 0.001$; $F(1,361) = 33.76$, $p < 0.001$; $F(1,361) = 30.36$, $p < 0.001$, respectively].

We next examined levels of synaptophysin (presynaptic markers) and PSD95 (postsynaptic markers) using western blot. Results showed a significant reduction in synaptopsin and PSD95 in vehicle-KO mice, which was normalized in 7,8-DHF-KO mice (Fig. 3I, 3J and 3K). Two-way ANOVA of synaptophysin levels showed a genotype × treatment interaction [$F(1,28) = 4.354$, $p = 0.046$], a main effect of genotype [$F(1,28) = 8.314$, $p = 0.008$], and a main effect of treatment [$F(1,28) = 6.858$, $p = 0.014$]. Two-way ANOVA of PSD95 levels showed a genotype × treatment interaction [$F(1,28) = 4.400$, $p = 0.045$], a main effect of treatment [$F(1,28) = 6.173$, $p = 0.019$], and no main effect of genotype. In all, these results suggest that 7,8-DHF treatment recovered abnormal synaptic structure in the hippocampus of *Fmr1* KO mice.

Given its effect on synaptic structure, we next exaimined whether 7,8-DHF restored synaptic plasticity in *Fmr1* KO mice. We tested low-frequency stimulation (LFS)- induced long-term depression (LTD) in each mice group, and observed significantly larger LTD in vehicle-KO than in vehicle-WT mice (87.24 ± 3.66% of baseline vs 62.07 ± 1.59% of baseline, $df = 8$, $t = 6.308$, $p < 0.001$, Fig. 4A and 4B). Whereas 7,8-DHF reduced LTD magnitude in KO mice (52.04 ± 6.63% of baseline, $df = 8$, $t = 4.649$, $P = 0.002$, compared to vehicle group, Fig. 4A and 4B) but showed no effect in LTD in WT mice (55.12 ± 6.56% of baseline, $df = 8$, $t = 1.030$, $P = 0.333$). Thus, 7,8-DHF appeared to rescue LTD deficit in *Fmr1* KO mice with no significant impact on WT mice. No significant difference in hippocampal LTP was observed in WT and *Fmr1* KO mice (data not shown). Taken together, synaptic structure and synaptic plasticity in *Fmr1* KO mice were restored by BDNF mimic and TrkB agonist, 7,8-DHF, suggest BDNF-TrkB dysregulation in *Fmr1* KO mice is the underlying mechanism of synaptic development.

Learning and memory deficits in Fmr1 **KO mice were rescued by TrkB agonist 7,8-DHF**

We first investigated the rescue effect in hippocampus-dependent learning and memory of 7,8-DHF, Morris water maze (MWM) was tested on 2-month-old *Fmr1* KO mice. The learning phase lasted 5 days. Two-way ANOVA of escape latency showed a main effect of genotype [F (1,44) = 9.71, p = 0.003], treatment [F (1,44) = 6.521, p = 0.014], and genotype×treatment interaction [F (1,44) = 5.512, p = 0.024]. During the learning phase (Fig. 5A), *Fmr1* KO mice showed significantly longer escape latencies, which suggested impaired spatial memory acquisition. 7,8-DHF-KO mice located the hidden platform more quickly than vehicle-KO mice. In fact, 7, 8-DHF restored the performance of KO mice to the level of vehicle-WT mice (Fig. 5A). After 5 days of training sessions, the probe test was used to evaluate spatial memory by measuring the time spent in the correct quadrant after the removal of the hidden platform. Two-way ANOVA of time spending and platform crossings in the target quadrant showed a main effect of genotype [F (1,44) = 9.857, p = 0.003; F (1,44) = 20.61, p < 0.001], treatment [F (1,44) = 7.118, p = 0.011; F(1,44) = 10.05, p = 0.003], and genotype×treatment interaction [F (1,44) = 5.932, p = 0.019; F(1,44) = 17.45, p < 0.001]. Vehicle-KO mice showed no preference for the correct quadrant and less platform crossings, whereas 7, 8-DHF-KO mice spent more time in the correct quadrant and crossed the previous location of the hidden platform as frequently as vehicle-WT mice did (Fig. 5B and 5C). In the visible-platform test, comparable motor and visual functions were observed among the four groups (Fig. 5D and 5E). Two-way ANOVA of escape latency and swimming speed showed no effect of genotype [F (1,44) = 0.0003, not significant (ns); F (1,44) = 0.80, ns], treatment [F (1,44) = 0.528, ns; F(1,44) = 0.0003, ns], or genotype×treatment interaction [F (1,44) = 1.236, ns; F(1,44) = 0.515, ns]. Therefore, variations in vision ability and swimming speeds did not cause behavioral differences among the groups.

We next tested whether 7,8-DHF normalizes the fear memory deficiencies in *Fmr1* KO mice. In fear conditioning test, 7,8-DHF showed a significant main effect of genotype [Hb: F (1, 36) = 0.9259, ns; CS-US1: F(1,36) = 0.182, ns; CS-US2: F(1,36) = 22.37, p < 0.001; CS-US3: F(1,36) = 11.94, p = 0.002] and treatment [Hb: F (1, 36) = 0.3707, ns;CS-US1: F(1,36) = 0.021, ns; CS-US2: F(1,36) = 13.23, p < 0.001; CS-US3: F(1,36) = 5.581, p = 0.024] as well as significant interactions [F(1, 36) = 0.160, ns; CS-US1: F(1,36) = 0.087, ns; CS-US2: F(1,36) = 10.82, p = 0.002; CS-US3: F(1,36) = 7.200, p = 0.011] with fear acquisition in the training session. Freezing time in vehicle-KO mice was significantly lower compared to vehicle-WT mice during the second and third tone-shock pairs (Fig. 6A). During inter-trial intervals, Vehicle-KO mice showed significantly less freezing time (Fig. 6B). Vehicle-KO mice also exhibited less freezing time when tested 24h later for contextual fear and 48h later for cued fear (Fig. 6C and Fig. 6D). In 7,8-DHF-KO mice, freezing time was normalized in the training session (Fig. 6B), the contextual fear test (Fig. 6C), and the cued fear test (Fig. 6D).

Discussion

The present study was designed to test the effect of early therapeutic intervention on morphological and behavioral phenotypes in young FXS mice and to explore the underlying neural molecular mechanisms. Our results showed that early treatment of 7,8-DHF, a TrkB agonist, was capable of ameliorating neuronal morphology and function in *Fmr1* KO mice and successfully improved their memory performance (Fig. 7). The activating of BDNF-TrkB-PLCγ/CaMK signaling pathway, as evidenced by the dramatic increases in

phosphorylated TrkB (Tyr816), PLCγ, and CaMK in hippocampus and primary cultured neurons, contributed to this pharmaceutical effect. These findings adding to existed evidence suggest that pharmaceutical treatment with TrkB agonist 7,8-DHF is effective strategy for FXS, and further provide the optimal window during the early developmental stages for therapeutic intervention.

Evidence tends to support the view that early intervention for ASD must be implemented during developmentally critical period preferably before major symptoms such as social communication disorders develop [42, 20]. Research findings have also demonstrated that early psychopharmacological and environmental intervention improve cognitive impairment in young FXS individuals [28]. Early developmental stage is the key period for highly reorganized brain structure and function, formation of newborn neural circuits and synaptic connections [24]. The treatment that miss this window may have limited effects. For example, early pharmacological intervention with mavoglurant exhibited more effective behavior improvement in the 0–3 days post fertilization in the zebrafish model of FXS, however, missing the optimal time window have irreversible consequences [43]. Early treatment with lovastatin exhibited lasting correct alteration of associative learning deficits for at least 14 weeks in FXS rat model, indicating the prevention of cognitive deficits and long-lasting benefits on cognition after early and transient therapeutic intervention [23]. In our study, FXS mice treated with 7,8-DHF starting at P14 showed long lasting improvements in the cognitive performances and synaptic function as still observed at 8 weeks after treatment, indicating the therapeutic intervention at early postnatal ages is essential and effective.

Recently, treatments with 7,8-DHF rescued object location memory and normalized LTP in adult (3 to 5-month-old) *Fmr1* KO mice [44]. Our previous study also reported that activation of TrkB through chronic oral administration of 7,8-DHF is able to rescue dendritic spine phenotypes and attenuate behavioral abnormalities in *Fmr1* KO mice [5]. The present study further examined BDNF-TrkB signaling's role in early developmental period of *Fmr1* KO mice, i.e. P14-P30. In order to avoid the inestimable oral dose for unweaned mice at postnatal developmental stages, the mice received repeated intraperitoneal injections of 7,8-DHF for 16 consecutive days. Consistently, we found that TrkB activation by intraperitoneal injection of 7,8-DHF had beneficial effects on *Fmr1* KO mice but no effect on the WT mice, which suggests that at the appropriate dose of 7,8-DHF can treat FXS-specific pathological conditions. Intriguingly, *in vitro* application of 7,8-DHF in cultured hippocampal neurons also promoted neuronal dendritic development, suggesting the supporting role of 7,8-DHF on *in vitro* neuron development.

As known, BDNF specific receptor TrkB is activated by autophosphorylation of its tyrosine residues, causing multiple intracellular signaling activation [14]. We therefore identified the specific signal pathway of 7,8-DHF acting by both *in vivo* and *in vitro.* We found that $TrkB^{Y816}$ phosphorylation but not $TrkB^{Y515}$ phosphorylation increased along with the induction of p-PLCγ and p-CaMKII after 7,8-DHF treatment, indicating that the TrkB-PLCγ-CaMKII pathway was responsible for the rescue by 7,8-DHF in *Fmr1* KO mice. These results are consistent with our previous report on the reduced activation of $TrkB^{Y816}$ phosphorylation and PLCγ-CaMKII in *Fmr1* KO mice and unchanged ERK pathway in the hippocampus of *Fmr1* KO mice with or without 7,8-DHF and enriched environment treatment [5, 19]. With $TrkB^{Y515}$

phosphorylation, two main pathways occured: the PI3K-AKT pathway and MAPK/ERK pathway, which activate anti-apoptotic effects and protein translation respectively [45]. With $TrkB^{Y816}$ phosphorylation, the PLCγ pathway is engaged, causing diacylglycerol production, increase in intracellular calcium, and the PKC and CAMK activation [46]. Seese et al. showed that 7,8-DHF increases synaptic TrkB phosphorylated at its Y515 site for activation of the ERK1/2 signaling pathway, in turn, may have effectors related to actin dynamics and learning [44].Whereas in this study, $TrkB^{Y816}$ phosphorylation was increased, through the activation of TrkB-PLCγ-CaMKII signaling pathway by 7,8-DHF treatment, we observed modulating changes in the spine dysmorphogenesis and abnormal synaptic function in *Fmr1* KO mice, and subsequently, an improvement in hippocampus-dependent learning and spatial and fear memory, as determined by MWM and conditional fear test.

In summary, we have been able to demonstrate that early intervention by TrkB stimulation with 7,8-DHF helps to establish and maintain the neural development and restore normal cognitive development in FXS. Further in-depth investigation of the understanding effective mechanisms for early intervention is warranted and will help develop future targeted treatments for FXS individuals.

Declarations

Acknowledgments

This work was supported by grants from National Natural Science Foundation of China (NSFC, grant nos. 82071272, 81571095 and 81870901).

Author Contribution

Yushan Chen and Yan Zeng conceived the idea, designed the project and wrote the manuscript. Siming Zhang, Qiong Zhu, Chaoxiong Yue, Peng Xiang performed the experiments and analyzed the data. Jinquan Li, Zhen Wei assisted with experiments and data analysis.

Funding

This work was supported by grants from National Natural Science Foundation of China (NSFC, grant nos. 82071272, 81571095 and 81870901).

Conflict of Interest The authors declare no competing interests.

Data Availability Authors will provide the data under a reasonable request.

Ethics Approval All procedures were approved by the Wuhan University of Science and Technology (WUST, Wuhan, China) ethics committee with the number IACUC-2017032.

Consent to participate Not applicable.

Consent for publication All authors read and approved the final manuscript.

References

1. Hagerman RJ, Berry-Kravis E, Hazlett HC, Bailey DB Jr, Moine H, Kooy RF, Tassone F, Gantois I, Sonenberg N, Mandel JL, Hagerman PJ (2017) Fragile X syndrome. Nat reviews Disease primers 3:17065. doi:10.1038/nrdp.2017.65
2. Hagerman RJ, Hagerman PJ (2022) Fragile X Syndrome: Lessons Learned and What New Treatment Avenues Are on the Horizon. Annu Rev Pharmacol Toxicol 62:365–381. doi:10.1146/annurev-pharmtox-052120-090147
3. Richter JD, Zhao X (2021) The molecular biology of FMRP: new insights into fragile X syndrome. Nat Rev Neurosci 22(4):209–222. doi:10.1038/s41583-021-00432-0
4. Wan RP, Zhou LT, Yang HX, Zhou YT, Ye SH, Zhao QH, Gao MM, Liao WP, Yi YH, Long YS (2017) Involvement of FMRP in Primary MicroRNA Processing via Enhancing Drosha Translation. Mol Neurobiol 54(4):2585–2594. doi:10.1007/s12035-016-9855-9
5. Tian M, Zeng Y, Hu Y, Yuan X, Liu S, Li J, Lu P, Sun Y, Gao L, Fu D, Li Y, Wang S, McClintock SM (2015) 7, 8-Dihydroxyflavone induces synapse expression of AMPA GluA1 and ameliorates cognitive and spine abnormalities in a mouse model of fragile X syndrome. Neuropharmacology 89:43–53. doi:10.1016/j.neuropharm.2014.09.006
6. Ferrante A, Boussadia Z, Borreca A, Mallozzi C, Pedini G, Pacini L, Pezzola A, Armida M, Vincenzi F, Varani K, Bagni C, Popoli P, Martire A (2021) Adenosine A(2A) receptor inhibition reduces synaptic and cognitive hippocampal alterations in Fmr1 KO mice. Transl Psychiatry 11(1):112. doi:10.1038/s41398-021-01238-5
7. Pyronneau A, He Q, Hwang JY, Porch M, Contractor A, Zukin RS (2017) Aberrant Rac1-cofilin signaling mediates defects in dendritic spines, synaptic function, and sensory perception in fragile X syndrome. Sci Signal 10(504). doi:10.1126/scisignal.aan0852
8. Gross C, Banerjee A, Tiwari D, Longo F, White AR, Allen AG, Schroeder-Carter LM, Krzeski JC, Elsayed NA, Puckett R, Klann E, Rivero RA, Gourley SL, Bassell GJ (2019) Isoform-selective phosphoinositide 3-kinase inhibition ameliorates a broad range of fragile X syndrome-associated deficits in a mouse model. Neuropsychopharmacology 44(2):324–333. doi:10.1038/s41386-018-0150-5
9. He CX, Portera-Cailliau C (2013) The trouble with spines in fragile X syndrome: density, maturity and plasticity. Neuroscience 251:120–128. doi:10.1016/j.neuroscience.2012.03.049
10. Chapleau CA, Larimore JL, Theibert A, Pozzo-Miller L (2009) Modulation of dendritic spine development and plasticity by BDNF and vesicular trafficking: fundamental roles in neurodevelopmental disorders associated with mental retardation and autism. J neurodevelopmental disorders 1(3):185–196. doi:10.1007/s11689-009-9027-6
11. Waterhouse EG, Xu B (2009) New insights into the role of brain-derived neurotrophic factor in synaptic plasticity. Mol Cell Neurosci 42(2):81–89. doi:10.1016/j.mcn.2009.06.009
12. Almeida LE, Roby CD, Krueger BK (2014) Increased BDNF expression in fetal brain in the valproic acid model of autism. Mol Cell Neurosci 59:57–62. doi:10.1016/j.mcn.2014.01.007

13. Zagrebelsky M, Korte M (2014) Form follows function: BDNF and its involvement in sculpting the function and structure of synapses. Neuropharmacol 76 Pt C 628–638. doi:10.1016/j.neuropharm.2013.05.029
14. Gottmann K, Mittmann T, Lessmann V (2009) BDNF signaling in the formation, maturation and plasticity of glutamatergic and GABAergic synapses. Exp Brain Res 199(3–4):203–234. doi:10.1007/s00221-009-1994-z
15. Luine V, Frankfurt M (2013) Interactions between estradiol, BDNF and dendritic spines in promoting memory. Neuroscience 239:34–45. doi:10.1016/j.neuroscience.2012.10.019
16. Castren ML, Castren E (2014) BDNF in fragile X syndrome. Neuropharmacol 76 Pt C 729–736. doi:10.1016/j.neuropharm.2013.05.018
17. Louhivuori V, Vicario A, Uutela M, Rantamaki T, Louhivuori LM, Castren E, Tongiorgi E, Akerman KE, Castren ML (2011) BDNF and TrkB in neuronal differentiation of Fmr1-knockout mouse. Neurobiol Dis 41(2):469–480. doi:10.1016/j.nbd.2010.10.018
18. Castren M, Lampinen KE, Miettinen R, Koponen E, Sipola I, Bakker CE, Oostra BA, Castren E (2002) BDNF regulates the expression of fragile X mental retardation protein mRNA in the hippocampus. Neurobiol Dis 11(1):221–229
19. Chen YS, Zhang SM, Yue CX, Xiang P, Li JQ, Wei Z, Xu L, Zeng Y (2022) Early environmental enrichment for autism spectrum disorder Fmr1 mice models has positive behavioral and molecular effects. Exp Neurol 114033. doi:10.1016/j.expneurol.2022.114033
20. Dawson G (2008) Early behavioral intervention, brain plasticity, and the prevention of autism spectrum disorder. Dev Psychopathol 20(3):775–803. doi:10.1017/s0954579408000370
21. Singer B, Friedman E, Seeman T, Fava GA, Ryff CD (2005) Protective environments and health status: cross-talk between human and animal studies. Neurobiol Aging 26 Suppl 1113–118. doi:10.1016/j.neurobiolaging.2005.08.020
22. Meredith RM (2015) Sensitive and critical periods during neurotypical and aberrant neurodevelopment: a framework for neurodevelopmental disorders. Neurosci Biobehav Rev 50:180–188. doi:10.1016/j.neubiorev.2014.12.001
23. Asiminas A, Jackson AD, Louros SR, Till SM, Spano T, Dando O, Bear MF, Chattarji S, Hardingham GE, Osterweil EK, Wyllie DJA, Wood ER, Kind PC (2019) Sustained correction of associative learning deficits after brief, early treatment in a rat model of Fragile X Syndrome. Sci Transl Med 11(494). doi:10.1126/scitranslmed.aao0498
24. Sullivan K, Stone WL, Dawson G (2014) Potential neural mechanisms underlying the effectiveness of early intervention for children with autism spectrum disorder. Res Dev Disabil 35(11):2921–2932. doi:10.1016/j.ridd.2014.07.027
25. Liu C, Wang Y, Deng J, Lin J, Hu C, Li Q, Xu X (2021) Social Deficits and Repetitive Behaviors Are Improved by Early Postnatal Low-Dose VPA Intervention in a Novel shank3-Deficient Zebrafish Model. Front Neurosci 15:682054. doi:10.3389/fnins.2021.682054

26. Su T, Fan HX, Jiang T, Sun WW, Den WY, Gao MM, Chen SQ, Zhao QH, Yi YH (2011) Early continuous inhibition of group 1 mGlu signaling partially rescues dendritic spine abnormalities in the Fmr1 knockout mouse model for fragile X syndrome. Psychopharmacology 215(2):291–300. doi:10.1007/s00213-010-2130-2
27. Kurtz PF, Chin MD, Robinson AN, O'Connor JT, Hagopian LP (2015) Functional analysis and treatment of problem behavior exhibited by children with fragile X syndrome. Res Dev Disabil 43–44:150–166. doi:10.1016/j.ridd.2015.06.010
28. Winarni TI, Schneider A, Borodyanskara M, Hagerman RJ (2012) Early intervention combined with targeted treatment promotes cognitive and behavioral improvements in young children with fragile x syndrome. Case Rep Genet 2012:280813. doi:10.1155/2012/280813
29. Thurman AJ, Potter LA, Kim K, Tassone F, Banasik A, Potter SN, Bullard L, Nguyen V, McDuffie A, Hagerman R, Abbeduto L (2020) Controlled trial of lovastatin combined with an open-label treatment of a parent-implemented language intervention in youth with fragile X syndrome. J Neurodev Disord 12(1):12. doi:10.1186/s11689-020-09315-4
30. Reichow B, Hume K, Barton EE, Boyd BA (2018) Early intensive behavioral intervention (EIBI) for young children with autism spectrum disorders (ASD). Cochrane Database Syst Rev 5(5):Cd009260. doi:10.1002/14651858.CD009260.pub3
31. Beaudoin GM 3, Lee SH, Singh D, Yuan Y, Ng YG, Reichardt LF, Arikkath J (2012) Culturing pyramidal neurons from the early postnatal mouse hippocampus and cortex. Nat Protoc 7(9):1741–1754. doi:10.1038/nprot.2012.099
32. Cheng K, Chen YS, Yue CX, Zhang SM, Pei YP, Cheng GR, Liu D, Xu L, Dong HX, Zeng Y (2019) Calsyntenin-1 Negatively Regulates ICAM5 Accumulation in Postsynaptic Membrane and Influences Dendritic Spine Maturation in a Mouse Model of Fragile X Syndrome. Front Neurosci 13:1098. doi:10.3389/fnins.2019.01098
33. Bian WJ, Miao WY, He SJ, Qiu Z, Yu X (2015) Coordinated Spine Pruning and Maturation Mediated by Inter-Spine Competition for Cadherin/Catenin Complexes. Cell 162(4):808–822. doi:10.1016/j.cell.2015.07.018
34. Yue C, Li J, Jin H, Hua K, Zhou W, Wang Y, Cheng G, Liu D, Xu L, Chen Y, Zeng Y (2019) Autophagy Is a Defense Mechanism Inhibiting Invasion and Inflammation During High-Virulent Haemophilus parasuis Infection in PK-15 Cells. Front Cell Infect Microbiol 9:93. doi:10.3389/fcimb.2019.00093
35. Sanz-García A, Knafo S, Pereda-Pérez I, Esteban JA, Venero C, Armario A (2016) Administration of the TrkB receptor agonist 7,8-dihydroxyflavone prevents traumatic stress-induced spatial memory deficits and changes in synaptic plasticity. Hippocampus 26(9):1179–1188. doi:10.1002/hipo.22599
36. Pei YP, Wang YY, Liu D, Lei HY, Yang ZH, Zhang ZW, Han M, Cheng K, Chen YS, Li JQ, Cheng GR, Xu L, Wu QM, McClintock SM, Yang Y, Zhang Y, Zeng Y (2020) ICAM5 as a Novel Target for Treating Cognitive Impairment in Fragile X Syndrome. J Neurosci 40(6):1355–1365. doi:10.1523/jneurosci.2626-18.2019

37. Huang CW, Hsieh YJ, Tsai JJ, Huang CC (2006) Effects of lamotrigine on field potentials, propagation, and long-term potentiation in rat prefrontal cortex in multi-electrode recording. J Neurosci Res 83(6):1141–1150. doi:10.1002/jnr.20797
38. Chatterjee M, Kurup PK, Lundbye CJ, Hugger Toft AK, Kwon J, Benedict J, Kamceva M, Banke TG, Lombroso PJ (2018) STEP inhibition reverses behavioral, electrophysiologic, and synaptic abnormalities in Fmr1 KO mice. Neuropharmacology 128:43–53. doi:10.1016/j.neuropharm.2017.09.026
39. Arias-Cavieres A, Barrientos GC, Sánchez G, Elgueta C, Muñoz P, Hidalgo C (2018) Ryanodine Receptor-Mediated Calcium Release Has a Key Role in Hippocampal LTD Induction. Front Cell Neurosci 12:403. doi:10.3389/fncel.2018.00403
40. Zhang B, Wang L, Chen T, Hong J, Sha S, Wang J, Xiao H, Chen L (2017) Sigma-1 receptor deficiency reduces GABAergic inhibition in the basolateral amygdala leading to LTD impairment and depressive-like behaviors. Neuropharmacology 116:387–398. doi:10.1016/j.neuropharm.2017.01.014
41. Lee KJ, Jung JG, Arii T, Imoto K, Rhyu IJ (2007) Morphological changes in dendritic spines of Purkinje cells associated with motor learning. Neurobiol Learn Mem 88(4):445–450. doi:10.1016/j.nlm.2007.06.001
42. Abubakar A, Kipkemoi P (2022) Early intervention in autism spectrum disorder: The need for an international approach. Dev Med Child Neurol 64(9):1051–1058. doi:10.1111/dmcn.15327
43. Medishetti R, Rani R, Kavati S, Mahilkar A, Akella V, Saxena U, Kulkarni P, Sevilimedu A (2020) A DNAzyme based knockdown model for Fragile-X syndrome in zebrafish reveals a critical window for therapeutic intervention. J Pharmacol Toxicol Methods 101:106656. doi:10.1016/j.vascn.2019.106656
44. Seese RR, Le AA, Wang K, Cox CD, Lynch G, Gall CM (2020) A TrkB agonist and ampakine rescue synaptic plasticity and multiple forms of memory in a mouse model of intellectual disability. Neurobiol Dis 134:104604. doi:10.1016/j.nbd.2019.104604
45. Yoshii A, Constantine-Paton M (2010) Postsynaptic BDNF-TrkB signaling in synapse maturation, plasticity, and disease. Dev Neurobiol 70(5):304–322. doi:10.1002/dneu.20765
46. Emili M, Guidi S, Uguagliati B, Giacomini A, Bartesaghi R, Stagni F (2022) Treatment with the flavonoid 7,8-Dihydroxyflavone: a promising strategy for a constellation of body and brain disorders. Crit Rev Food Sci Nutr 62(1):13–50. doi:10.1080/10408398.2020.1810625

Figures

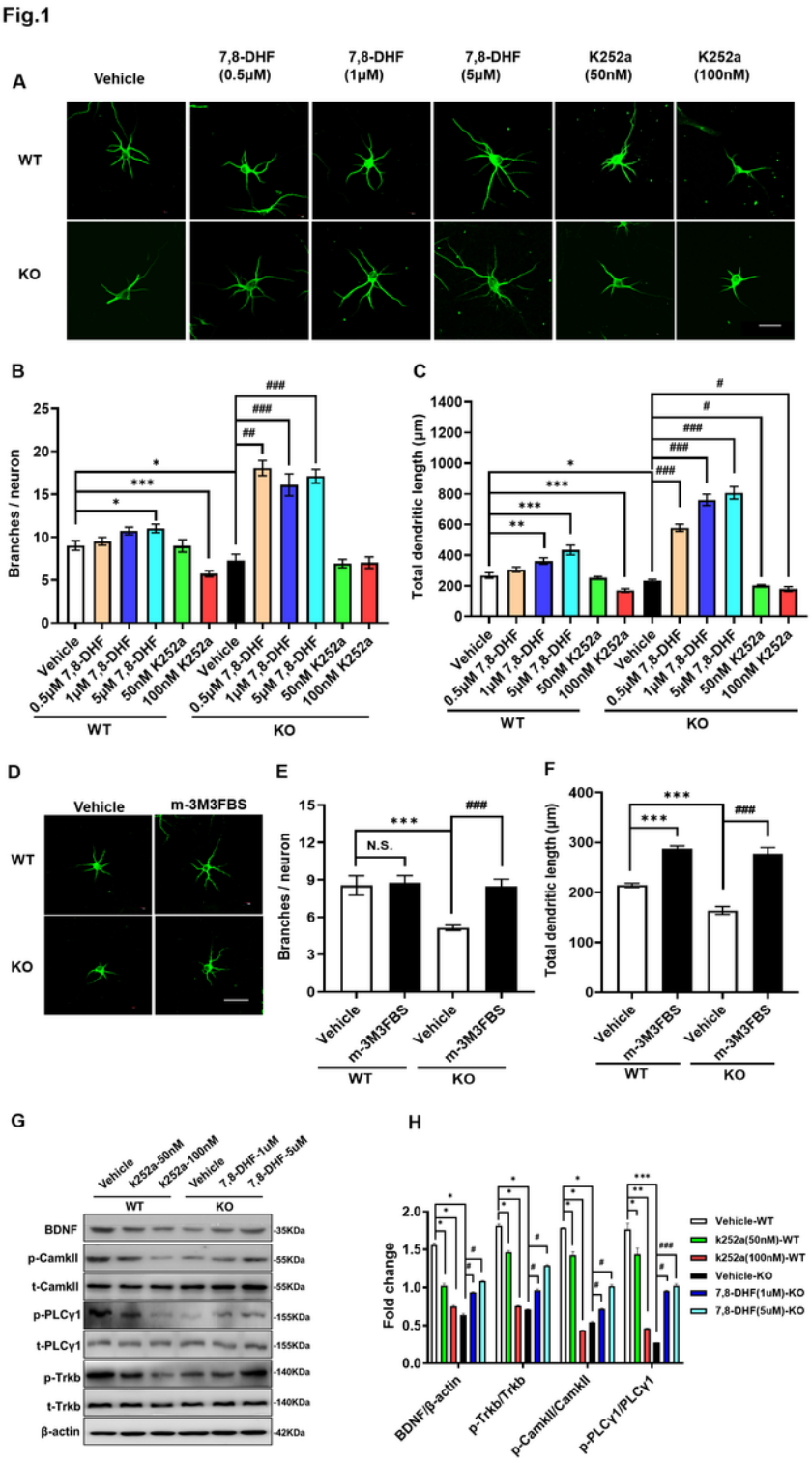

Figure 1

7,8-DHF improves hippocampal neuronal morphology caused by *Fmr1* deficiency *in vitro*.

(A) Primary neurons were treated with 7,8-DHF (0.5 μM, 1 μM, or 5 μM) at DIV 4 for 3 days or K252a (50 nM or 100 nM) at DIV 6 for 24h. Representative images of DIV 7 cultures stained with MAP2. Scale bar= 30 μm. Quantification of **(B)** dendritic branches and **(C)** total dendritic length in neuron cultures. **(D)**

Primary neurons were treated with PLCγ agonist m-3M3FBS (25 μM) at DIV 5 for 1h and then staining with MAP2. Quantification of **(E)** dendritic branches and **(F)** total dendritic length in neuron cultures. n=5 independent cultures per group ×10 images per culture. (**G** and **H)** Western blots analysis of BDNF, phosphorylated and total TrkB, PLC-γ, CaMKII (n=3). Mean and SEM are shown. **P*<0.05, ***P*<0.01, ***P*<0.001 vs vehicle-WT; $^{\#}P$<0.05, $^{\#\#}P$<0.01, $^{\#\#\#}P$<0.001 vs vehicle-KO. N.S., not significant.

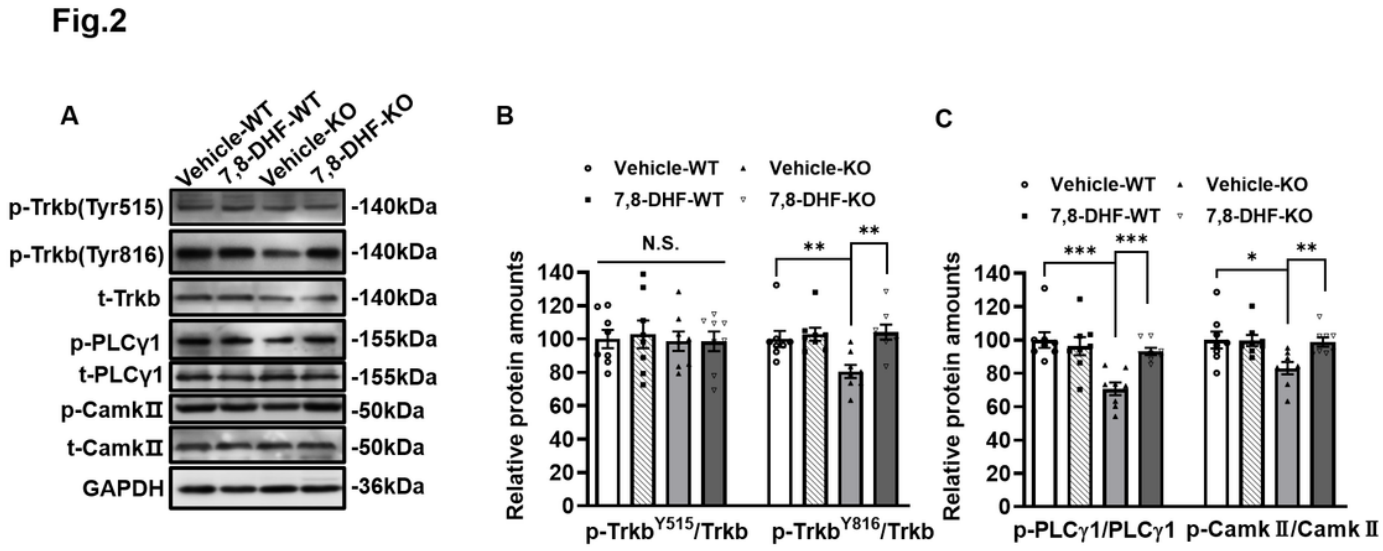

Figure 2

Effects of 7,8-DHF intraperitoneal injection on BDNF downstream signaling in the hippocampus of WT and *Fmr1* KO mice.

(A and D) Representative Western blots showing immunoreactivity for total and phosphorylated TrkB, PLC-γ, CaMKII. Data in **(B)** were normalized to TrkB; data in **(C)** were normalized to PLC-γ and CaMKII, respectively; n = 8, Data are shown as mean ± SEM. **P* < 0.05, ***P* < 0.01, ****P* < 0.001 vs vehicle-KO.

Fig.3

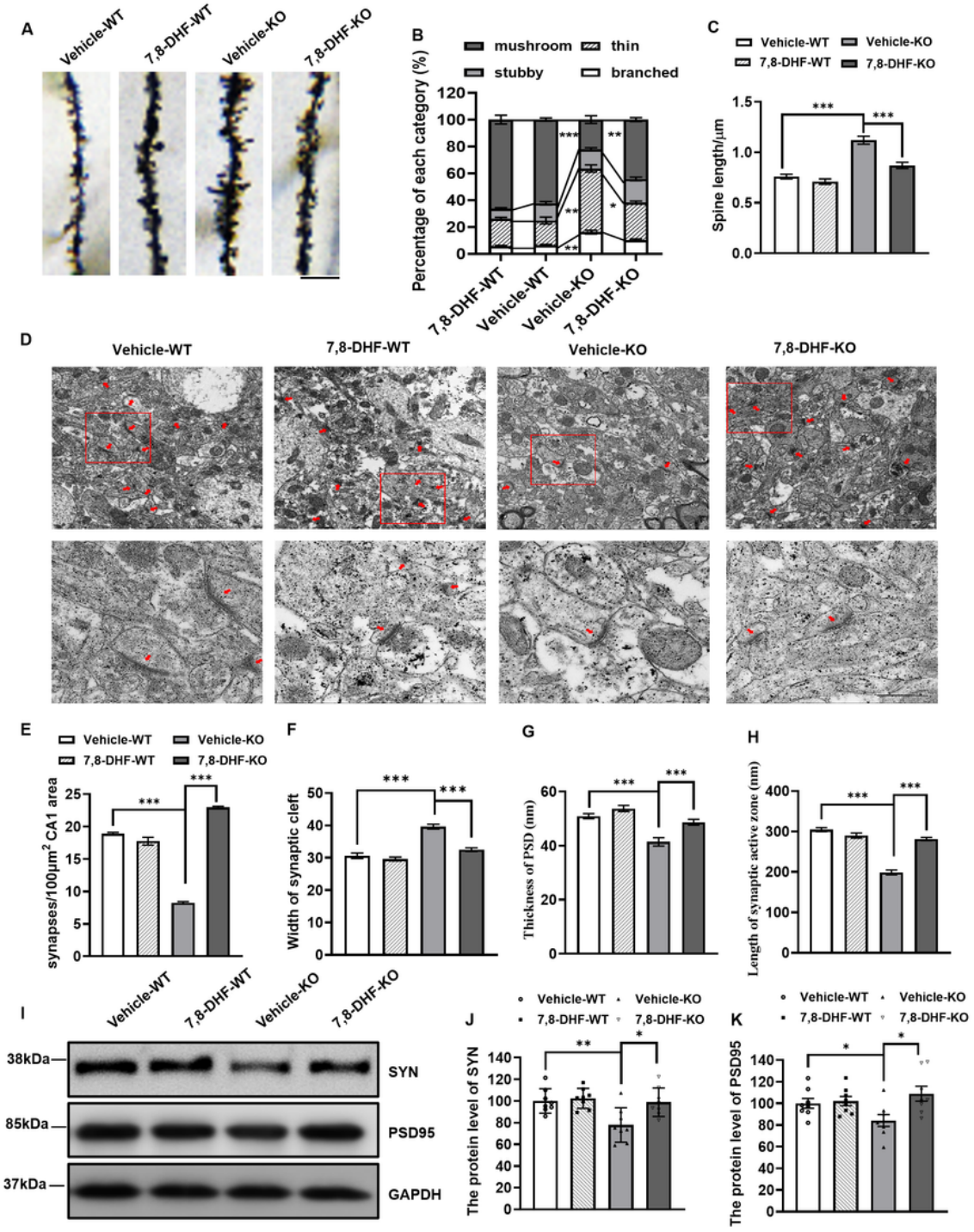

Figure 3

Effects of 7,8-DHF intraperitoneal injection on dendritic spine density, synaptic structure, and protein levels of synaptophysin and PSD95 in the hippocampus CA1 of WT and *Fmr1*KO mice.

(A) Photomicrograph of dendrites in CA1 pyramidal neurons of WT and *Fmr1* KO mice. Scale bar=5 μm.
(B) Percentages of each category (mushroom, stubby, thin and branched) of spines in pyramidal neurons

per group. Error bars show SEM in all results. n = 5 mice per group, 3-8 neurons per mouse, 1 segments per neuron. *p< 0.05, **p < 0.01, ***p < 0.001. **(C)** Quantification of spine length (spines per μm) on basal dendrites in the CA1 region. n = 5 mice per group, 3-8 neurons per mouse, 5 segments per neuron. ***p< 0.001. **(D)** Schematic representatiion of CA1 area in hippocampus. Bar chart showing **(E)** density of synapses, **(F)** thickness of postsynaptic density (PSD), **(G)** width of the synaptic cleft, **(H)**length of the synaptic active zone (Scale bar: 1 or 0.5 μm). n = 5 per group. Data presented mean ± SEM. ***p < 0.001 vs vehicle-KO. **(I)** The protein levels of synaptophysin (SYN) and PSD95 detected by Western blot in hippocampus. SYP **(J)** and PSD95 **(K)** levels were normalized to GAPDH and expressed as fold difference. n = 8 mice per group. Values are mean ± SEM. *P< 0.05, **P < 0.01 vs vehicle-KO.

Fig.4

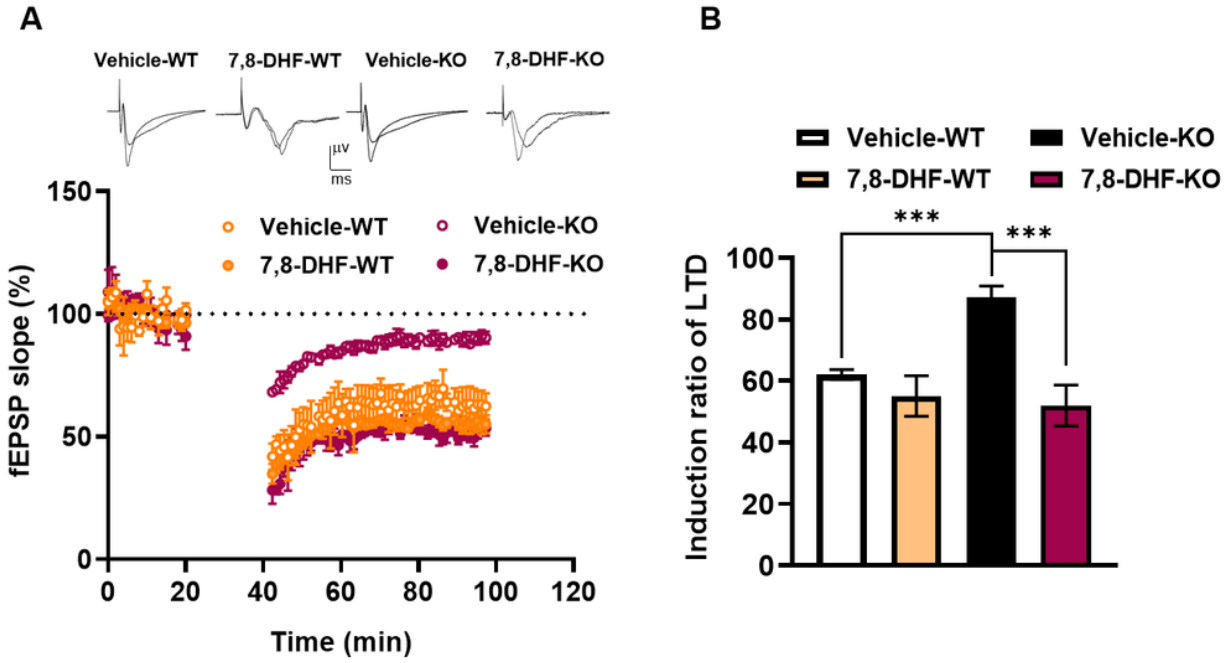

Figure 4

Effects of 7,8-DHF intraperitoneal injection on synaptic plasticity in the hippocampus.

(A) Low-frequency stimulation induced LTD was measured in CA1 in slices prepared from vehicle-WT, vehicle-KO, 7,8-DHF-WT, and 7,8-DHF-KO mice. Figure shows the time course of the mean field excitatory postsynaptic potential (fEPSP) slope. n = 5 slices/5 mice. **(B)** Induction ratios of LTD. Mean and SEM are shown. ***P < 0.001.

Fig.5

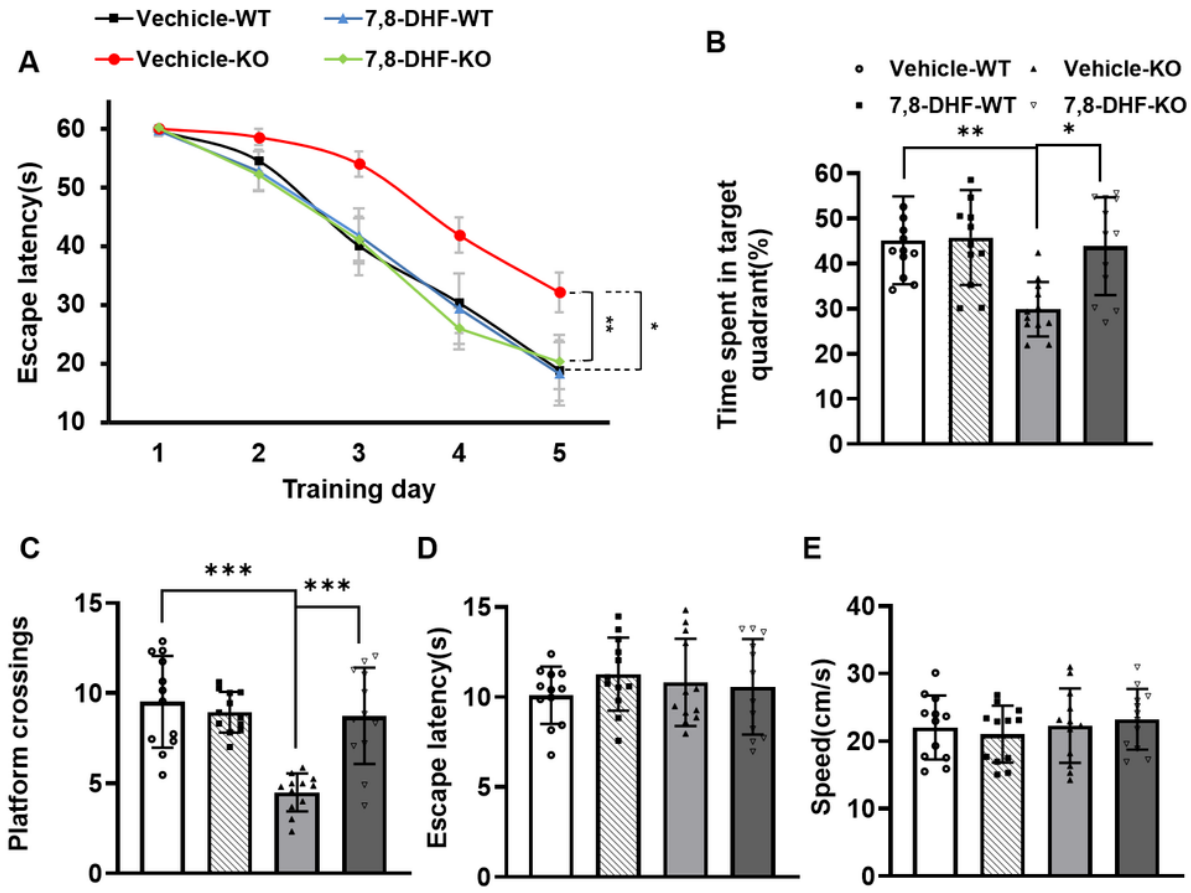

Figure 5

Effect of 7,8-DHF intraperitoneal injection on spatial learning and memory in *Fmr1* KO mice in the MWM test.

(A) Means of escape latency from day 1 to day 5 of the training test (hidden platform trials). **(B)**Time spent in the target quadrant during the probe trial test. **(C)** The number of platform crossings. There was no significant difference in the latency **(D)** and in swimming speed **(E)** among different animal groups. Error bars show SEM in all results. n = 12 mice per group. **p< 0.01, ***p < 0.001vs vehicle-KO.

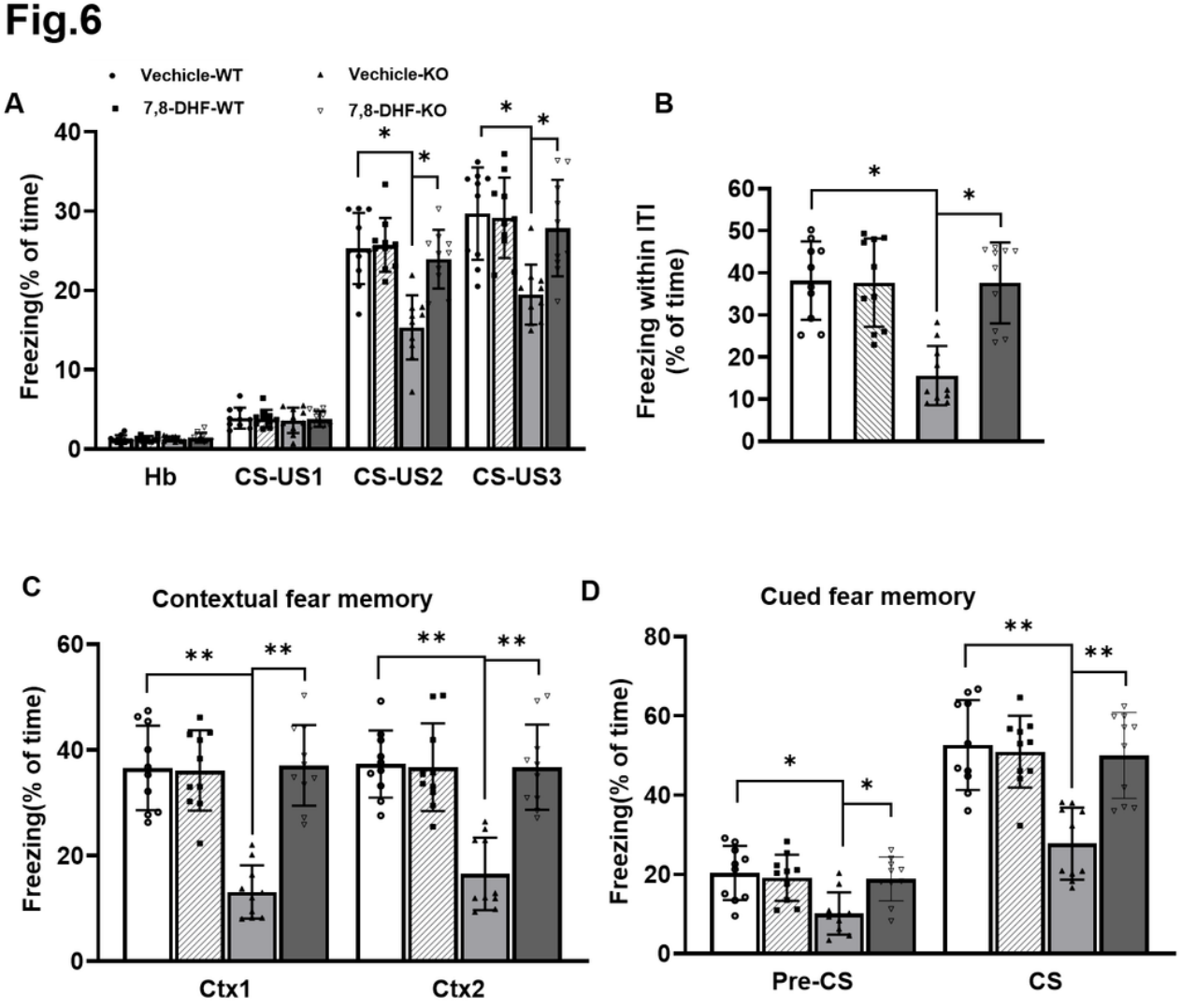

Figure 6

Effect of 7,8-DHF intraperitoneal injection on fear memory in *Fmr1* KO mice.

Mice were submitted to a training session and exposed to the context with or without receiving electrical foot shock. **(A)** Freezing time of mice from associative CS-US pairings. **(B)** Average freezing time during intertrial intervals (ITI). **(C** and **D)** Freezing time in contextual fear condition and in cued fear condition. Error bars show SEM. n = 10 mice per group. *$p < 0.05$, **$p < 0.01$ vs vehicle-KO.

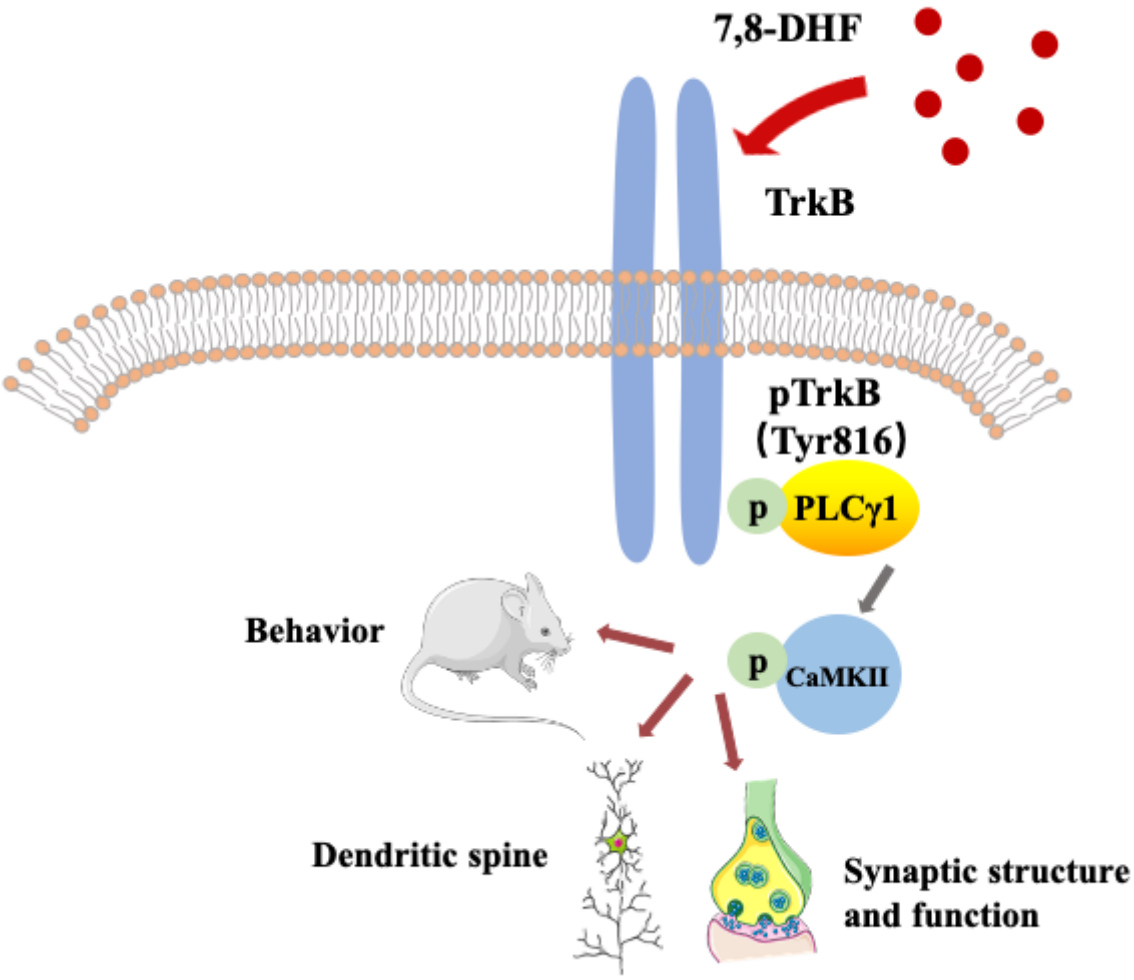

Figure 7

Schematic illustration: 7,8-Dihydroxyflavone administration ameliorates synaptic structure and function, neuronal dendritic spine and behavioral deficits in the young FXS mice by activating BDNF-TrkB-PLC-γ-CaMKII pathway.

Supplementary Files

This is a list of supplementary files associated with this preprint. Click to download.

- TableS1.docx